Convergence acceleration and stabilization of dynamical mean-field theory calculations

Rok Žitko
Jožef Stefan Institute, Jamova 39, SI-1000 Ljubljana, Slovenia

(Received 1 June 2009; revised manuscript received 2 September 2009; published 25 September 2009)

The convergence to the self-consistency in the dynamical mean-field theory (DMFT) calculations for models of correlated electron systems can be significantly accelerated by using an appropriate mixing of hybridization functions which are used as the input to the impurity solver. It is shown that the techniques and the past experience with the mixing of input charge densities in the density-functional theory calculations are also effective in DMFT. As an example, the increase in the computational requirements near the Mott metal-insulator transition in the Hubbard model due to critical slowing down can be strongly reduced by using the modified Broyden's method to numerically solve the nonlinear self-consistency equation. Speed-up factors as high as three were observed in practical calculations even for this relatively well-behaved problem. Furthermore, the convergence can be achieved in difficult cases where simple linear mixing is either not effective or even leads to divergence. Unstable and metastable solutions can also be obtained. We also determine the linear response of the system with respect to the variations in the hybridization function, which is related to the propagation of the information between the different energy scales during the iteration.

DOI: 10.1103/PhysRevB.80.125125 PACS number(s): 71.27.+a, 71.30.+h, 72.15.Qm, 02.60.Cb

I. INTRODUCTION

In many transition-metal, lanthanide, and actinide compounds the almost-localized d and f orbitals are partially filled and local magnetic moments are formed at low temperatures.[1,2] The competition between itinerancy and local electron-electron correlation effects gives rise to complex phase diagrams with different magnetic, charge ordered, and superconducting phases.[1–6] Simplified tight-binding models with short-range Coulomb interaction terms are commonly used to study strong-correlation effects in such systems. In the paradigmatic Hubbard model,[7–10] the problem is reduced to a single-orbital description with purely on-site Coulomb repulsion. Hubbard-type models are thought to correctly describe certain aspects of the itinerant ferromagnetism, the metal-insulator transitions,[1,11] and the high-temperature superconductivity.[3,12] Despite intensive research, the properties of the Hubbard model are not yet fully established. In the limit of infinite dimensions or high lattice connectivity the problem can be solved by the dynamical mean-field theory (DMFT).[13–22] In this limit, the self-energy becomes purely local and the bulk problem of correlated electrons maps exactly onto a quantum impurity model with a self-consistently defined noninteracting bath of conduction electrons. In the DMFT, the spatial correlations are described in a mean-field way, however, the local quantum fluctuations are taken into account exactly; as long as the effect under study is driven by local physics, the results of DMFT calculations are a good approximation for the properties of real (finite-dimensional) materials.

In spite of the significant simplification of the full problem within the DMFT, the solution of the effective quantum impurity problem is still challenging: it is by far the most computationally demanding part of the calculations. Among several impurity solvers in common use, the numerical renormalization group (NRG) (Refs. 23–30) is distinguished by its applicability to study the regime of very low temperatures directly in the thermodynamic limit. The convergence-acceleration approach proposed in the following is clearly applicable to any impurity solver that may be used to solve the DMFT problem, however, the discussion, the implementation details, and the test results are given for the NRG. Nevertheless, the technique can easily be adapted for other solvers in a straightforward manner.

The input to a NRG calculation is the hybridization function $\Gamma(\omega)$ which contains information about the density of states (DOS) of the effective medium into which the impurity is embedded, while the output is an impurity spectral function $A(\omega)$, which is then used to compute the local lattice spectral function $\rho(\omega)$. The self-consistency is achieved when the two become equal, i.e., $A(\omega)=\rho(\omega)$ within chosen accuracy, otherwise $\rho(\omega)$ is used to compute new hybridization function for the next DMFT iteration. In order to ensure the convergence, in some situations $\Gamma(\omega)$ from two consecutive iterations are linearly mixed to obtain the hybridization function which is used as the input to the NRG. A similar situation is well known in the field of quantum chemistry and electronic-structure calculations, in particular, in the density-functional theory (DFT) (Refs. 31–33) where the quantity to be mixed is the charge density in space, $n(\mathbf{r})$. In difficult cases (metallic surfaces, heterostructures, impurities in metals, systems near magnetic instabilities, etc.), the simple linear mixing procedure converges too slowly (or not at all), thus more sophisticated mixing approaches were devised.[34] In these schemes, a system of nonlinear equations is solved iteratively by quasi-Newton-Raphson procedures or similar methods.[34–47] The solution of the system is equivalent to the Kohn-Sham variational principle.[48] Such "advanced mixing" techniques are implemented with various degrees of sophistication in all DFT packages. They are stable, easy to implement and use, and they often have very high convergence rate.

In this paper it is shown that the techniques and the past experience with the advanced mixing schemes in DFT calculations can also be applied to DMFT calculations. The advanced mixing greatly accelerates the convergence in many cases, for example, near the Mott metal-insulator transition,

where the iteration converges very slowly due to critical slowing down. It also ensures the convergence to unstable and metastable solutions, hence it can be applied to situations with multiple coexisting solutions.

This work is structured as follows. In Sec. II the DMFT self-consistency constraint is formulated as a sufficient condition in the form of a system of equations. In Sec. III the modified Broyden's iterative method for solving systems of nonlinear equations is briefly described, focusing on the implementation with low storage requirements which is more suitable for large-scale problems.[38] In Sec. IV it is shown how the Broyden solver is incorporated into the DMFT loop and some further implementation details are given. In Sec. V the convergence properties of the linear and advanced mixing schemes are compared on the example of the Hubbard model for increasing electron-electron repulsion U. In Sec. VI the Hubbard model in external magnetic field is considered; in this case, the simple mixing is not always successful and the use of Broyden's method was found to be essential to obtain rapid convergence. In Sec. VII we study the response of the Hubbard model with respect to small variations in the hybridization function; this response function is the equivalent of the Jacobian matrix of the system of self-consistency equations and describes the propagation of the information between various energy scales during the DMFT iteration. Finally, in Sec. VIII some examples of the stabilization of otherwise unstable fixed-point solutions are discussed.

II. DMFT SELF-CONSISTENCY CONSTRAINT AS A SYSTEM OF NONLINEAR EQUATIONS

The single-orbital Hubbard model[7,8] for electrons on a d-dimensional lattice

$$H = \sum_{\langle ij\rangle,\sigma} t_{i,j} c^{\dagger}_{i,\sigma} c_{j,\sigma} - \sum_{i,\sigma} \mu_{\sigma} n_{i,\sigma} + U \sum_{i} n_{i,\uparrow} n_{i,\downarrow} \tag{1}$$

[with $n_{i,\sigma}=c^{\dagger}_{i,\sigma}c_{i,\sigma}$ and $\mu_{\sigma}=\mu-(\sigma/2)g\mu_B B$] maps in the $d \to \infty$ limit[16,18,21] onto the single-impurity Anderson model (SIAM) (Ref. 49)

$$H_{\mathrm{SIAM}} = \epsilon_{d,\sigma} n + U n_{\uparrow} n_{\downarrow} + \sum_{k,\sigma} (V_{k,\sigma} c^{\dagger}_{k,\sigma} d_{\sigma} + \mathrm{H.c.}) + \sum_{k,\sigma} \epsilon_{k,\sigma} c^{\dagger}_{k,\sigma} c_{k,\sigma} \tag{2}$$

with $n_{\sigma}=d^{\dagger}_{\sigma}d_{\sigma}$ and $n=n_{\uparrow}+n_{\downarrow}$. The hybridization function $\Gamma_{\sigma}(\omega)=\Sigma_k |V_{k,\sigma}|^2 \delta(\omega-\epsilon_{k,\sigma})$ contains full information about the coupling between the impurity and the effective noninteracting medium. From the calculated impurity spectral function

$$A_{\sigma}(\omega) = -\frac{1}{\pi}\mathrm{Im}[G_{\sigma}(\omega + i\delta)], \tag{3}$$

where $G_{\sigma}(z)=\langle\langle d_{\sigma}; d^{\dagger}_{\sigma}\rangle\rangle_z$ is the impurity Green's function, one can extract the interaction self-energy $\Sigma_{\sigma}(\omega)$ defined through

$$G_{\sigma}(\omega) = \frac{1}{\omega - \epsilon_{d,\sigma} + \Delta_{\sigma}(\omega) - \Sigma_{\sigma}(\omega)}, \tag{4}$$

where $\mathrm{Im}\,\Delta_{\sigma}(\omega)=\Gamma_{\sigma}(\omega)$ and the real part of $\Delta_{\sigma}(\omega)$ can be obtained via the Kramers-Kronig transformation. In practice, the self-energy can be calculated more reliably and accurately as the ratio of two correlation functions:[26] the generalized Green's function $F_{\sigma}(z)=\langle\langle d_{\sigma} n_{\bar{\sigma}}; d^{\dagger}_{\sigma}\rangle\rangle_z$ over the Green's function $G_{\sigma}(z)$, i.e., $\Sigma_{\sigma}(\omega)=UF_{\sigma}(\omega)/G_{\sigma}(\omega)$. The local lattice Green's function is

$$G_{\mathrm{loc},\sigma}(\omega) = \frac{1}{N}\sum_{k} G_{k,\sigma}(\omega) \tag{5}$$

$$= \frac{1}{N}\sum_{k} \frac{1}{[\omega + \mu_{\sigma} - \Sigma_{\sigma}(\omega)] - \epsilon_k} \tag{6}$$

$$= \int \frac{\rho_0(\epsilon) d\epsilon}{[\omega + \mu_{\sigma} - \Sigma_{\sigma}(\omega)] - \epsilon}, \tag{7}$$

where $\rho_0(\epsilon)$ is the DOS in the noninteracting model. The local lattice spectral function is then

$$\rho_{\sigma}(\omega) = -\frac{1}{\pi}\mathrm{Im}[G_{\mathrm{loc},\sigma}(\omega + i\delta)]. \tag{8}$$

The self-consistency condition[16] relates the local lattice Green's function $G_{\mathrm{loc},\sigma}$ and the hybridization function Γ_{σ} as

$$\Gamma_{\sigma}(\omega) = -\mathrm{Im}[\omega - \mathcal{G}^{-1}_{0,\sigma}(\omega)], \tag{9}$$

$$\mathcal{G}^{-1}_{0,\sigma}(\omega) = G^{-1}_{\mathrm{loc},\sigma} + \Sigma_{\sigma}(\omega). \tag{10}$$

One DMFT cycle (which involves the numerical solution of H_{SIAM}, the calculation of $G_{\mathrm{loc},\sigma}$, and the determination of the new hybridization function Γ_{σ} via Eq. (9) can be considered as a functional of the input hybridization function, i.e.,

$$\Gamma^{\mathrm{new}}_{\sigma} = \Gamma^{\mathrm{new}}_{\sigma}\{\Gamma^{\mathrm{old}}(\omega)\}. \tag{11}$$

If the self-consistency has been established, the hybridization function is invariant (fixed point)

$$\Gamma^{\mathrm{new}}_{\sigma}\{\Gamma^{\mathrm{old}}_{\sigma}(\omega)\} = \Gamma^{\mathrm{old}}_{\sigma}. \tag{12}$$

Defining a mapping F as the difference

$$F(\Gamma_{\sigma}) = \Gamma^{\mathrm{new}}_{\sigma}\{\Gamma_{\sigma}\} - \Gamma_{\sigma}, \tag{13}$$

the approach to the self-consistency clearly corresponds to solving the system of equations

$$F(\Gamma_{\sigma}) = 0, \tag{14}$$

while a single DMFT step corresponds to applying F once to the hybridization function. Any solution of the Eq. (14) is a possible physical state of the system since it satisfies the self-consistency condition, albeit it is not necessarily the ground state: solutions corresponding to unstable and metastable states can also be found (see Sec. VIII). It should be noted that Eq. (14) is highly nonlinear.

The usual DMFT iteration with no mixing corresponds to solving Eq. (14) by a direct iteration, which often works since the mapping F behaves as a contraction in the vicinity of the solution (and often even far away from it). When F is not a contraction, however, this procedure will tend to diverge and more care is required. Usually it is sufficient to take an average of two hybridization functions (the current and the previous one)

$$\Gamma^{\text{input},(m)} = \alpha\Gamma^{\text{new},(m)} + (1-\alpha)\Gamma^{\text{input},(m-1)}, \tag{15}$$

where $\alpha \in [0:1]$ is the mixing parameter. It should be remarked that this is fully analogous to simple charge mixing in the density-functional theory, where the charge density from the previous iteration $n^{\text{old}}(\mathbf{r})$ is admixed to the current one $n^{\text{new}}(\mathbf{r})$ as the true input to the next DFT iteration. Unfortunately, there are situations where this simple linear mixing approach fails even for small values of α. Furthermore, for very small α the approach to the self-consistency becomes prohibitively slow. In such situations, more sophisticated mixing approaches are required. In DFT, Broyden's method is commonly used.

III. BROYDEN'S METHOD

Let $\mathbf{V}$ be an N-dimensional vector and F a mapping; the goal is to solve the system of equations $F(\mathbf{V})=0$. The quasi-Newton-Raphson methods are iterative techniques in which the new approximation is given by

$$\mathbf{V}^{(m+1)} = \mathbf{V}^{(m)} - [J^{(m)}]^{-1}\mathbf{F}^{(m)}, \tag{16}$$

where $J^{(m)}$ is the Jacobian of the system at point $\mathbf{V}^{(m)}$ and $\mathbf{F}^{(m)}=F(\mathbf{V}^{(m)})$. The true Jacobian is unknown; a simple approximation is used for the initial Jacobian, for example, a constant diagonal matrix

$$J^{(1)} = -\frac{1}{\alpha}\mathbf{1}, \tag{17}$$

which corresponds to simple linear mixing with a mixing parameter $\alpha \in [0:1]$. The approximation is then improved by performing rank-1 updates as the iteration proceeds. It is more efficient to update directly the inverse of the Jacobian $B^{(m)}=-[J^{(m)}]^{-1}$ as[35,37]

$$B^{(m+1)} = B^{(m)} + (\Delta\mathbf{V}^{(m)} - B^{(m)}\Delta\mathbf{F}^{(m)}) \otimes \Delta\mathbf{F}^{(m)}, \tag{18}$$

where

$$\Delta\mathbf{V}^{(m)} = \frac{\mathbf{V}^{(m+1)} - \mathbf{V}^{(m)}}{|\mathbf{F}^{(m+1)} - \mathbf{F}^{(m)}|}, \tag{19}$$

$$\Delta\mathbf{F}^{(m)} = \frac{\mathbf{F}^{(m+1)} - \mathbf{F}^{(m)}}{|\mathbf{F}^{(m+1)} - \mathbf{F}^{(m)}|}. \tag{20}$$

Vanderbilt and Louie have proposed a modified version of Broyden's method in which the information from all previous iterations is incorporated when the current Jacobian is updated; this approach has better convergence properties and the Jacobian converges to the true Jacobian, which is not the case in the original Broyden's method which only uses the information from the most recent iteration to perform the update.[36] Srivastava has simplified the computational scheme so that only the input vectors $\mathbf{V}^{(m)}$ and output vectors $\mathbf{F}^{(m)}$ need to be stored, rather than the complete Jacobian matrix.[37] Johnson combined the advantages of both schemes without any increase in complexity.[38] The final expressions for this modified Broyden's method are as follows:

$$\mathbf{V}^{(m+1)} = \mathbf{V}^{(m)} + \alpha\mathbf{F}^{(m)} - \sum_{n=1}^{m-1}\sum_{k=1}^{m-1} w_n w_k c_k^{(m)} \beta_{k,n}^{(m)} \mathbf{U}^{(n)} \tag{21}$$

with

$$c_k^{(m)} = (\Delta\mathbf{F}^{(k)})^{\dagger}\mathbf{F}^{(m)}, \tag{22}$$

$$\mathbf{U}^{(n)} = \alpha\Delta\mathbf{F}^{(n)} + \Delta\mathbf{V}^{(n)}, \tag{23}$$

and $(m-1)\times(m-1)$-dimensional matrices

$$\beta_{k,n}^{(m)} = [(w_0^2\mathbf{1} + A^{(m)})^{-1}]_{k,n}, \tag{24}$$

$$A_{k,n}^{(m)} = w_k w_n (\Delta\mathbf{F}^{(n)})^{\dagger}\Delta\mathbf{F}^{(k)}. \tag{25}$$

Here $\mathbf{1}$ is a $(m-1)\times(m-1)$-dimensional identity matrix. The first two terms in Eq. (21) correspond to simple linear mixing with parameter α, as described above, while the final term is a correction which takes into account the updates to the initial Jacobian.

The weights $w_n (n=1,2,\ldots)$ are usually chosen to be equal to 1, while $w_0=0.01$.[38,40] For a suitable choice of weights, the modified Broyden's method becomes equivalent[39,45] to Pulay mixing scheme[42] or Anderson mixing scheme.[44]

The algorithm can be simply modified to use only a finite number of previous iterations to update the vector. This may be advantageous when the initial approximation for the vector is not very good. Alternatively, the Broyden mixing can be fully restarted after a given number of iterations.

IV. INCORPORATION OF THE BROYDEN SOLVER INTO THE DMFT LOOP

In the proposed convergence acceleration scheme for DMFT, the modified Broyden's method is used to refine the hybridization function $\Gamma(\omega)$ which is used as the input to the impurity solver. It should be remarked that this is not the only possibility: alternatively, one could also mix the self-energy $\Sigma(\omega)$. The choice depends somewhat on the problem and for numerical reasons one should in extreme cases preferably choose the quantity which is smoother as a function of the energy (for example, near the Mott transition on the metallic side the self-energy features sharp peaks while the hybridization function is rather smooth, whereas in the antiferromagnetic phase with small U the hybridization function contains sharp inverse-square-root singularities while the self-energy is relatively smooth). In general, however, the two approaches are expected to be nearly equivalent.

The Broyden solver is called just before the NRG, see Fig. 1. In a sense, the Broyden solver is effectively driving the DMFT loop in order to solve the equation

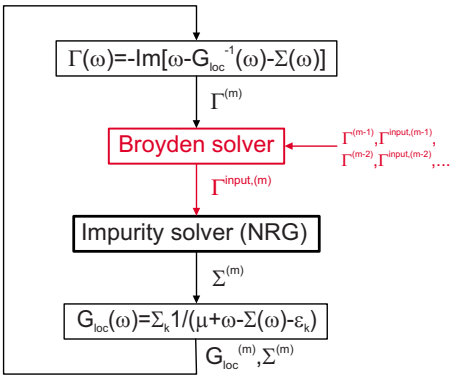

FIG. 1. (Color online) The DMFT loop using the numerical renormalization group as the impurity solver. The Broyden solver is incorporated in the loop as a correction step which modifies the input hybridization function in order to accelerate the convergence to the self-consistency. The new elements in the loop are shown in gray (red online).

$$F\{\Gamma^{\mathrm{input},(m)}\} = \Gamma^{(m+1)}\{\Gamma^{\mathrm{input},(m)}\} - \Gamma^{\mathrm{input},(m)} = 0, \qquad (26)$$

see also Eqs. (13) and (14). One cycle of the loop thus corresponds to applying once the mapping F to the hybridization function.

The vector $\mathbf{V}^{(m)}$ corresponds to a discretized representation of the continuous function $\Gamma(\omega)$. In the calculations presented in this work, we used a geometric sequence of points $\omega_{\pm,n} = \pm\Omega_{\max} l^n$ with $\Omega_{\max}$ that exceeds the band width of the noninteracting band by a factor of order 10 and $l=1.01$; the dimension of the vectors was $N=3982$ (and twice as large for spin-dependent problems). The same grid is used to sample all other functions, in particular the impurity spectral function $A(\omega)$ and the self-energy $\Sigma(\omega)$. The Jacobian matrix in the Broyden solver was typically initialized with $\alpha=1$. The weights were chosen as $w_0=0.01$ and $w_n=1$ for $n\geq 1$; setting w_0 to zero was found to have little effect. It has been suggested that the weights w_n be chosen as $w_n=\langle \mathbf{F}^{(m)} | \mathbf{F}^{(m)} \rangle^{-1/2}$, i.e., as the inverse root-mean-square difference of the function.[38] Numerical tests have shown that the improvement is only minor, if at all existing.

During the initial steps it sometimes occurs that the resulting $\Gamma^{\mathrm{input}}(\omega)$ is not positive for all ω as the solver is overcompensating for the deviations. In such cases, the function was simply clipped to positive values. When the error vectors $\Delta\mathbf{F}$ become smaller as the iteration proceeds, this is no longer a problem. The clipping performed during the initial iterations does not affect the final result. An alternative solution would be to revert to simple linear mixing in such instances. Yet another possible approach to enforce positivity of Γ would consist of working with $\ln\Gamma$ instead. Unfortunately, this method was found to slow down the convergence significantly.

It is necessary to store both $\Gamma^{(m)}(\omega)$ and $\Gamma^{\mathrm{input},(m)}(\omega)$ for all N_{steps} DMFT steps, thus the additional storage requirements are on the order of $N\times N_{\mathrm{steps}}$, which is not likely to pose difficulty.

In calculations with fixed occupancy (rather than fixed chemical potential) it is important to store as an additional component of the vector $\mathbf{V}$ also the chemical potential μ that is being tuned. (This is actually true in general: all parameters varied in the iteration should appear in the Broyden process, so that the output of a single iteration is a smooth and uniquely defined function of the input vector $\mathbf{V}$ alone.[40]) In fact, the tuning of the parameter μ can be integrated in the Broyden solver with much fruition. This can be simply implemented by extending the dimensions of vectors $\mathbf{V}$ and $\mathbf{F}$ by one. In the additional element of $\mathbf{V}$ we store the chemical potential at the current iteration, while the additional element of $\mathbf{F}$ can be defined as $c(\langle n\rangle - n_{\mathrm{goal}})$, where c is some coefficient related to charge stiffness (but in practice it can usually be set to 1, since Broyden mixing will find an appropriate scale factor automatically as the iteration proceeds), $\langle n\rangle$ is the occupancy at the current DMFT iteration, while n_{goal} is the target occupancy that we seek to stabilize. The additional element in the new input vector $\mathbf{V}^{(m+1)}$ will then contain the chemical potential to be used in the new impurity solver step.

In the NRG calculations performed for testing the method and presented in the following, the z averaging[50–52] over $N_z=8$ values of the twist parameter was used in combination with an improved discretization scheme based on solving a differential equation to obtain the discretization coefficients.[53,54]The discretization parameter was $\Lambda=2$, the truncation cutoff was set to $E_{\mathrm{cutoff}}=10\omega_N$ (but no less than 500 and no more than 10000 states were used) and care was taken to truncate in a "gap" between clustered excitation levels. Spectral functions were computed using the density-matrix approach[55] and the self-energy trick.[26] Spectral information was extracted from both even and odd NRG iterations with a window parameter $p=2.3$.[53] The broadening procedure from Ref. 56 with $\alpha=0.1$ was used. The choice of NRG parameters appears to be important for the convergence: high-quality (smooth) results tend to be beneficial for the rate of convergence, while "rough" calculations sometimes lead to a stagnation of the convergence and oscillatory behavior. This is related to the assumption of differentiability of the mapping F. For the same reason, the calculations performed with larger broadening parameter will converge faster than high-energy-resolution calculations with much smaller broadening parameter. This is especially true when the hybridization function contains sharp features.

The DMFT loop is terminated when two consecutive impurity spectral functions $A(\omega)$ differ by no more than some chosen value:

$$\int |A^{(m)}(\omega) - A^{(m-1)}(\omega)| d\omega \leq \lambda. \qquad (27)$$

In practice it is found that this convergence test is more stringent when compared to an equivalent test for consecutive local lattice spectral functions $\rho(\omega)$, while comparing $A(\omega)$ and $\rho(\omega)$ at the same iteration gives absolute integrated errors somewhere between these two convergence tests. A typical convergence limit is $\lambda=10^{-6}$.

The stability of the converged solution can be tested by performing a few further DMFT iterations with the Broyden mixing turned off. From the solutions one can extract the

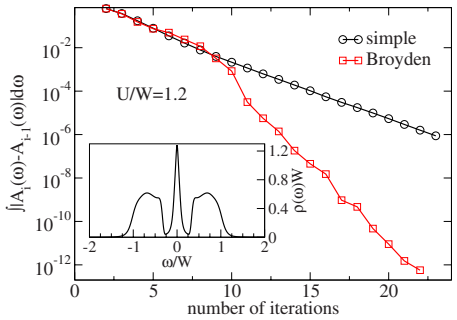

FIG. 2. (Color online) Comparison of the convergence of the impurity spectral function $A(\omega)$ in a calculation for the Hubbard model defined on the Bethe lattice in the paramagnetic phase at half-filling. We compare the simple mixing (here $\alpha=1$, i.e., the output from the previous iteration is used directly as the input for the new iteration, so this is actually direct iteration rather than mixing) and Broyden's mixing. The inset shows the converged density of states.

dominant eigenvalue and eigenvector of the mapping F. This information is instrumental in assessing the physical stability of the solution and to determine the type of eventual instability. We return to these considerations in Sec. VIII.

V. ACCELERATION OF THE CONVERGENCE

The acceleration of the convergence of the DMFT loop toward self-consistency was explored on the well-studied case of the Hubbard model at half-filling ($\mu=0$) in the paramagnetic regime.[16–19,22,26,27,29,21,57] We study the Hubbard model on the Bethe lattice with infinite coordination number where

$$\rho_0(\epsilon) = \frac{4}{\pi W}\sqrt{1-(2\epsilon/W)^2}. \tag{28}$$

Here W is the width of the noninteracting conduction band. As the electron-electron repulsion U is increased, the characteristic three-peak structure emerges: two Hubbard bands and a quasiparticle peak at the Fermi level. As U approaches a critical value of $U_c/W \approx 1.46$, the quasiparticle peak becomes increasingly narrow and disappears.[16,26,27,57] Recent high-energy-resolution calculations have confirmed that the Hubbard bands have inner structure, in particular a peak at the inner edges;[53,58,59] this structure can be observed, for example, in the inset in Fig. 2.

In Fig. 2 we compare the approach to the self-consistency for the Hubbard model at fixed $U/W=1.2$. The initial approximation for the local spectral function was the noninteracting DOS $\rho_0(\omega)$. Initially, both approaches are equivalent, since the starting approximation for the Jacobian is a diagonal matrix which corresponds to simple mixing. Since $\rho_0(\omega)$ is a rather crude approximation to the real density of states, Broyden's method is not expected to work much better than simple mixing for the first few steps; indeed, the errors are found to be even slightly higher. As can be seen in Fig. 3, the nonlinear Broyden corrections are initially especially large in the region of the emerging Hubbard bands, while at later

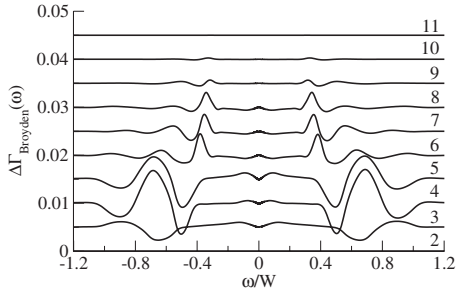

FIG. 3. The Broyden corrections for consecutive iterations; the curves are offset for clarity. The parameters are as in Fig. 2.

iterations the most important contributions are to the inner-edge peaks in the Hubbard bands. Starting with iteration 9, the approximation to the self-consistent hybridization function becomes quite adequate, the updates to the Jacobian correspond to accurate refinements and the convergence accelerates significantly. Both methods converge linearly, however, the rate of convergence is much faster with Broyden's method. Superlinear convergence was never observed in practice. The linear rate of convergence in the example shown in Fig. 2 was $\mu \approx 0.15$. When required, extremely good accuracy of the solution can thus be obtained with essentially no additional computational effort as compared to the direct iteration.

We also determined the speed-up due to using the modified Broyden's method as a function of the interaction strength U, Fig. 4. As the Mott metal-insulator transition is approached from below, the convergence becomes more difficult to achieve, which can be assigned to critical slowing down in the vicinity of quantum phase transitions.[27,60,61] Both approaches are affected by this difficulty, however, it is found that the relative speed up in Broyden's method is an increasing function of U; for the range of parameter U considered in this work, the speed up was up to a factor of 3 and it presumably increases even further for $U \to U_c$. It should be remarked that in these calculations it was possible to use $\alpha=1$ (in other words, the direct DMFT iteration converges without any mixing), which is the most favorable situation. In problems where mixing with small α is necessary, the speed-up factor is expected to be much higher.

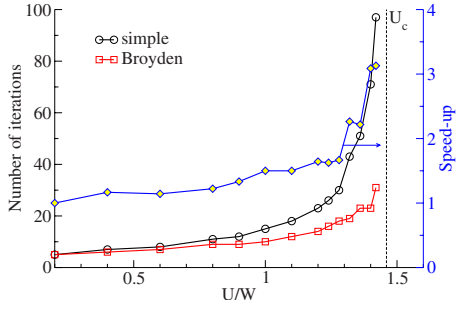

FIG. 4. (Color online) Comparison of the convergence as a function of the interaction strength U/W. The convergence is defined to occur when two consecutive solutions for the density of states differ by not more than $\lambda=10^{-6}$ (integrated absolute value of the difference). The vertical dashed line corresponds to the point of the Mott metal-insulator transition at $U_c/W=1.46$.

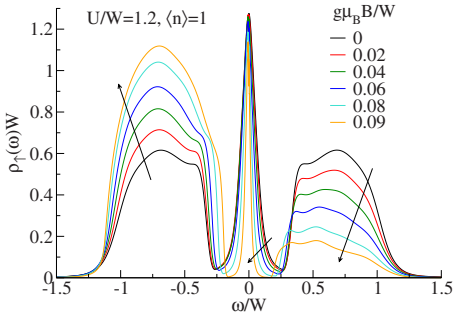

FIG. 5. (Color online) Majority-spin spectral functions for the half-filled Hubbard model in a magnetic field. The arrows show the direction of the increasing magnetic field.

By performing calculation in the close vicinity of the Mott transition on the metallic side, we obtained an improved estimate of the critical value of U

$$U_c/W = 1.459. \tag{29}$$

It agrees very well with previous NRG calculations, where $U_c/W=1.47$ was established,[27] and even better with the value obtained using projective self-consistent approach, $U_c/W=1.46$.[16,57]

VI. HUBBARD MODEL IN THE MAGNETIC FIELD

The Hubbard model in a strong magnetic field[62,63] has a metamagnetic response in a certain parameter regime: the magnetic susceptibility increases with the field strength.[16,62,64–66] The metamagnetic response is due to electron-electron interactions and, for sufficiently large U, it is driven mostly by field-induced quasiparticle mass enhancement (i.e., field-induced localization), however, quasiparticle interactions also play a role.[66]

We consider the Hubbard model at half-filling and at zero temperature in a magnetic field. This problem is interesting for several reasons: (1) it is found that a DMFT iteration with simple mixing (and taking the noninteracting DOS as an initial approximation) does not always converge in the presence of the magnetic field; (2) the structure at the inner edge of the Hubbard band might be of magnetic origin, thus it can have nontrivial behavior in a finite magnetic field;[53,58,59] and (3) the behavior near the threshold to full polarization is not fully understood due to numerical difficulties in the transition regime.[66]

The calculated spectral functions are presented in Fig. 5. The results agree with those shown in Ref. 66, however, the energy resolution in our approach is sufficiently higher so that the inner structure in the Hubbard bands may be resolved.[53] As already established, when the magnetic field is increased the quasiparticle peak shifts away from the Fermi level and it narrows down, and the spectral weight is gradually transferred to the lower Hubbard band of the majority spin.[66] With improved resolution, we can now also observe that the internal structure of the Hubbard bands changes significantly with increasing field. When the magnetic field is increased past a transition value B_c, a field-induced metal-insulator transition is induced.[66]

For a system in the metallic regime, the Broyden's method converged rapidly, even when the noninteracting DOS was taken as the initial approximation, while linear mixing usually led to oscillatory behavior. As in the Mott metal-insulator transition, the number of necessary iterations increases as the transition point is approached. On the insulating side, the convergence to the fully polarized solution was rapid for large fields, however, the calculations in the vicinity of the transition point were more difficult and it was necessary to initialize the problem with the fully polarized insulating spectral functions to ensure the convergence. The difficulties appear to stem from the fact that the noninteracting DOS for the Bethe lattice has square-root singularities at the band edges, while the Broyden method is premised on the differentiability of the mapping F.

The inner structure in the Hubbard bands remains present even in the presence of the magnetic field, see Fig. 5. With increasing field, the lower Hubbard band of the majority-spin electrons becomes increasingly featureless and the inner-edge peak tends to disappear as we approach the transition to the insulating phase. The upper Hubbard band, however, appears to become more structured and distinctively asymmetric. Even at low fields there is some hint of further weak peaks within this band, which become more pronounced in the vicinity of the transition. In this regime, the electrons are already strongly polarized, thus majority-spin electrons in the upper Hubbard band cannot easily propagate since they reside on doubly occupied sites surrounded predominantly by a ferromagnetic background, thus their motion is strongly hindered by the Pauli exclusion principle and they become increasingly localized. This is to be contrasted with the holes in the lower Hubbard band which can easily propagate and do not feel the strong electron-electron interactions.

VII. RESPONSE WITH RESPECT TO THE VARIATION IN THE INPUT HYBRIDIZATION FUNCTION

Finding a good initial approximation to the Jacobian is not trivial, therefore a simple diagonal constant matrix is typically used, as in Eq. (17). In band-structure calculations, the Jacobian is related to the dielectric tensor,[34,37,48] which makes it possible to devise an improved initial approximation for the Jacobian based on the Thomas-Fermi screening theory (this procedure is called "preconditioning").[34,37,43,46] The Jacobian for the hybridization function in the DMFT loop is not related to some well-understood physical quantity in a simple way [see, however, the discussion of the Landau-Ginzburg (LG) functional F_{LG} of the hybridization function discussed in Ref. 67 which is related to the self-consistency equation $F(\Gamma)=0$]. We may, however, study the properties of the Jacobian in the vicinity of the self-consistent solution $\Gamma^{sc}(\omega)$ by performing calculations with slightly perturbed input hybridization functions:

$$\Gamma^{\text{input}}(\omega) = \Gamma^{sc}(\omega) + a\frac{e^{-b^2/4}}{b\sqrt{\pi}}e^{-[\ln(\omega/E)/b]^2}. \tag{30}$$

The perturbation takes the form of a log-Gaussian function centered at the energy E and of width b, similar to the com-

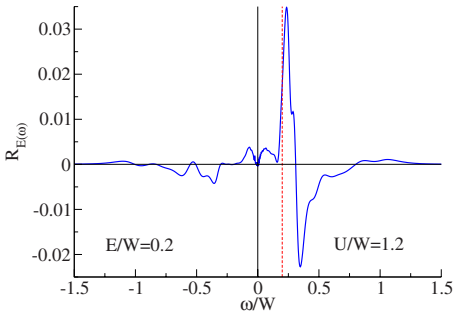

FIG. 6. (Color online) The response function $R_E(\omega)$ for the Hubbard model for the excitation energy $E/W=0.2$ (graphically represented as the vertical dashed line). Model parameters are the same as in Fig. 2.

monly used broadening kernel for producing smooth spectral functions in NRG (although the normalization factor differs).[29] The weight a should be chosen small enough so that the response function

$$R_E(\omega) = \frac{1}{a}[\Gamma^{\text{output}}(\omega) - \Gamma^{\text{sc}}(\omega)] \tag{31}$$

no longer depends on the value of a, but it must be large enough to prevent numerical artifacts. The width b should likewise be as small as possible, although its value is ultimately limited by the NRG broadening which restrains the energy resolution in $\Gamma^{\text{output}}(\omega)$. The calculations were performed for $a=0.001$ and $b=0.05$.

An example of the response function for the Hubbard model with intermediately strong interaction $U/W=1.2$ is shown in Fig. 6. It reveals that a variation at a given excitation energy E can lead to a complex response at all energies. [However $R_E(\omega)$ vanishes in the $\omega \to 0$ limit.[18]] In simple linear mixing there is no exchange of information between different energies ("crosstalk"), thus it takes many DMFT iterations for reaching the self-consistency after a change has been imposed. In the Broyden mixing, the application of the (approximate) Jacobian effectively mixes the hybridization function at different energies, thereby accelerating the propagation of the information.

VIII. UNSTABLE AND METASTABLE FIXED POINTS

The concept of self-consistency is inseparably related to the concept of iteration; this is directly implied by the form of the self-consistency Eq. (12). For this reason, the stability of the solutions (fixed points) is related to the eigenspectrum of the DMFT transformation, i.e., of the mapping F. Direct iteration can only be convergent if all the eigenvalues λ_i of the linearization of F in the vicinity of the fixed point are strictly less than 1 in absolute value, while it will diverge when one or several eigenvalues are larger than one in absolute value, unless the solution space is constrained in such a way that the initial approximation for the solution has no components along the directions of the corresponding eigenvectors. For linear mixing with parameter $\alpha \in [0:1]$ (note that $\alpha=1$ corresponds to direct iteration), the convergence criterium becomes[34]

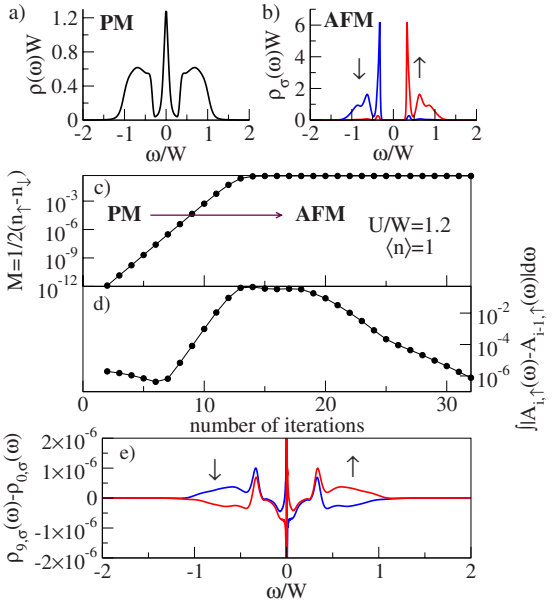

FIG. 7. (Color online) Evolution of the paramagnetic solution for the half-filled Hubbard model after switching off the Broyden mixing. (a) Initial paramagnetic spectral function. (b) Resulting antiferromagnetic spin-dependent spectral functions. (c) Magnetization and (d) convergence as a function of the number of iterations. (e) Difference between the spectral functions at iteration 9 and the initial spectral function indicating the progressive breaking of the spin symmetry.

$$|1 - \alpha(1 - \lambda_i)| < 1. \tag{32}$$

We denote by $\lambda_{\max}$ and $\lambda_{\min}$ the maximal and minimal eigenvalue. If $\lambda_{\max} < 1$ and $\lambda_{\min} > -1$, the direct iteration with $\alpha = 1$ will converge. If $\lambda_{\max} < 1$ and $\lambda_{\min} \leq -1$, α should be $\alpha < 2/(1-\lambda_{\min})$. Finally, if $\lambda_{\max} > 1$ the inequality Eq. (32) cannot be satisfied for any $\alpha \in [0:1]$ and the linear mixing is of no help, thus the use of advanced mixing schemes becomes mandatory.

As an example of a well-understood unstable solution, let us consider the instability of the paramagnetic solution of the Hubbard model at half-filling toward an antiferromagnetically ordered Néel ground state.[18,21,68,69] Using Broyden's method, the paramagnetic (PM) solution can be stabilized in a calculation which in principle allows a symmetry broken state. The system drifts away, however, from the PM fixed point as soon as the Broyden mixing is turned off and eventually it converges to an antiferromagnetic (AFM) solution, as illustrated in Fig. 7. The calculation was seeded with a previously obtained self-consistent PM solution and iterated further without Broyden solver. The magnetization immediately starts to increase [Fig. 7(c)] and by the tenth iteration the spectral functions develop a narrow but sizeable singularity structure (emerging spectral gap) in the quasiparticle peak, while the Hubbard bands start to become spin polarized [Fig. 7(e)]. After 32 iterations, the result converged within $\eta = 10^{-6}$ to a stable self-consistent AFM solution shown in Fig. 7(b).

It should be recalled that in a calculation where the SU(2) symmetry in spin space is explicitly maintained, the PM so-

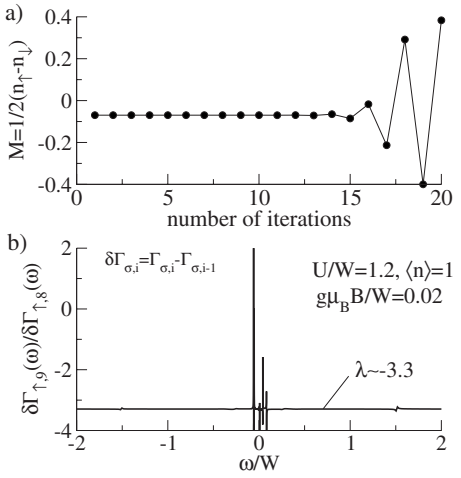

FIG. 8. Evolution of the solution for the Hubbard model at half-filling in an external magnetic field after switching off the Broyden mixing. (a) Magnetization as a function of the number of iterations, (b) ratio between the differences of consecutive hybridization functions, which provides an estimate for the dominant eigenvalue $\lambda \sim -3.3$ for $B/W=0.02$.

lution is stable and the mapping F is a contraction, as shown in Sec. V. The eigenspectrum of the mapping F is not only a property of the physical model under consideration, but it also depends on the type of the long-range order allowed for in the DMFT equations, and to some degree even on the impurity solver used and on other details of the calculation (spectral broadening, discretization parameter, number of states kept, etc.).

Another situation commonly encountered after switching off the Broyden mixing is the emergence of oscillatory solutions which never converge. This behavior can be observed for the Hubbard model at half-filling in a magnetic field (see Sec. VI). The polarized fixed-point solution are found to be unstable and lead to oscillations between two almost fully spin-polarized (in the opposite directions) spectral functions, see Fig. 8(a). The instability can be traced to a dominant eigenvalue of $\lambda \sim -3.3 < -1$ (for example, in Fig. 8), as extracted from the ratio of differences between consecutive hybridization functions in the vicinity of the fixed point, Fig. 8(b). This solution could thus be stabilized using linear mixing with $\alpha < 0.23$. It should be remarked that the solution was found to be unstable for all magnetic fields that yield a spin-polarized metallic solution, not only for weak fields where the system is known to be unstable toward the AFM solution. If the instability of the fixed point is a true physical instability also for large magnetic fields, its nature is not very clear; it might correspond to canted ferromagnetism, a tendency toward formation of spin-density waves, or some other kind of incommensurate order.[70] Since such states cannot be described by the formalism used, the iteration cannot converge.

Since the fixed points Γ^* of the self-consistency equation $F(\Gamma^*)=0$ are generally stationary points, rather than extrema,[67,71] it will be interesting to further clarify the relations between the stability of the DMFT iteration and the physical stability of the solution, as well as their relation to the eigenspectra of the mapping F in the vicinity of the solutions. As demonstrated, the proposed mixing technique can be a valuable tool for numerical studies of these questions, since it allows in principle to obtain all self-consistent solutions and (by turning the mixing off) to analyze the nature of their possible instabilities.

IX. CONCLUSION

It has been shown that the approach to the self-consistency can be greatly accelerated by reformulating the DMFT loop as an iterative method for solving a nonlinear self-consistency equation using quasi-Newton-Raphson methods. The tests performed for the paradigmatic case of the Hubbard model at half-filling have shown that Broyden's method significantly outperforms simple linear mixing. The approach is fully general and it can be also applied when any other impurity solver (such as, for example, exact diagonalization, DMRG, or quantum Monte Carlo) is used; it appears likely that similar speed-up factors could be achieved on equivalent problems. For particularly pathological situations, the improvement might be sufficient to bring previously forbidding problems within reach. This is particularly important near quantum phase transitions, where reaching the convergence becomes problematic due to critical slowing down and the detailed behavior at the transition points is still a matter of controversy for many important problems. The acceleration due to the use of Broyden's method might be instrumental in answering some of these long-standing questions. In addition, the solver can be used to stabilize unstable fixed-point solutions and to study their properties. Since the solver is robust, easy to implement and to incorporate in the DMFT cycle, there is little reason not to use it.

ACKNOWLEDGMENTS

Very fruitful discussions with Thomas Pruschke and Robert Peters are gratefully acknowledged.

[1] M. Imada, A. Fujimori, and Y. Tokura, Rev. Mod. Phys. **70**, 1039 (1998).
[2] A. C. Hewson, *The Kondo Problem to Heavy-Fermions* (Cambridge University Press, Cambridge, 1993).
[3] E. Dagotto, Rev. Mod. Phys. **66**, 763 (1994).
[4] M. B. Salamon and M. Jaime, Rev. Mod. Phys. **73**, 583 (2001).
[5] P. A. Lee, N. Nagaosa, and X.-G. Wen, Rev. Mod. Phys. **78**, 17 (2006).
[6] G. R. Stewart, Rev. Mod. Phys. **56**, 755 (1984).
[7] P. W. Anderson, Phys. Rev. **115**, 2 (1959).
[8] J. Hubbard, Proc. R. Soc. London **276**, 238 (1963).
[9] J. Kanamori, Prog. Theor. Phys. **30**, 275 (1963).

[10] M. C. Gutzwiller, Phys. Rev. Lett. **10**, 159 (1963).
[11] W. F. Brinkman and T. M. Rice, Phys. Rev. B **2**, 4302 (1970).
[12] P. W. Anderson, Science **235**, 1196 (1987).
[13] W. Metzner and D. Vollhardt, Phys. Rev. Lett. **62**, 324 (1989).
[14] T. Pruschke, M. Jarrell, and J. K. Freericks, Adv. Phys. **44**, 187 (1995).
[15] T. Maier, M. Jarrell, T. Pruschke, and M. H. Hettler, Rev. Mod. Phys. **77**, 1027 (2005).
[16] A. Georges, G. Kotliar, W. Krauth, and M. J. Rozenberg, Rev. Mod. Phys. **68**, 13 (1996).
[17] X. Y. Zhang, M. J. Rozenberg, and G. Kotliar, Phys. Rev. Lett. **70**, 1666 (1993).
[18] A. Georges and G. Kotliar, Phys. Rev. B **45**, 6479 (1992).
[19] M. J. Rozenberg, X. Y. Zhang, and G. Kotliar, Phys. Rev. Lett. **69**, 1236 (1992).
[20] E. Müller-Hartmann, Z. Phys. B: Condens. Matter **74**, 507 (1989).
[21] M. Jarrell, Phys. Rev. Lett. **69**, 168 (1992).
[22] O. Sakai and Y. Kuramoto, Solid State Commun. **89**, 307 (1994).
[23] K. G. Wilson, Rev. Mod. Phys. **47**, 773 (1975).
[24] H. R. Krishna-murthy, J. W. Wilkins, and K. G. Wilson, Phys. Rev. B **21**, 1003 (1980).
[25] O. Sakai, Y. Shimizu, and T. Kasuya, J. Phys. Soc. Jpn. **58**, 3666 (1989).
[26] R. Bulla, A. C. Hewson, and T. Pruschke, J. Phys.: Condens. Matter **10**, 8365 (1998).
[27] R. Bulla, Phys. Rev. Lett. **83**, 136 (1999).
[28] T. Pruschke, R. Bulla, and M. Jarrell, Phys. Rev. B **61**, 12799 (2000).
[29] R. Bulla, T. Costi, and T. Pruschke, Rev. Mod. Phys. **80**, 395 (2008).
[30] T. A. Costi, A. C. Hewson, and V. Zlatic, J. Phys.: Condens. Matter **6**, 2519 (1994).
[31] W. K. P. Hohenberg, Phys. Rev. **136**, B864 (1964).
[32] W. Kohn and L. J. Sham, Phys. Rev. **140**, A1133 (1965).
[33] R. M. Martin, *Electronic structure—Basic Theory and Practical Methods* (Cambridge University Press, Cambridge, 2004).
[34] P. H. Dederichs and R. Zeller, Phys. Rev. B **28**, 5462 (1983).
[35] C. G. Broyden, Math. Comput. **19**, 577 (1965).
[36] D. Vanderbilt and S. G. Louie, Phys. Rev. B **30**, 6118 (1984).
[37] G. P. Srivastava, J. Phys. A **17**, L317 (1984).
[38] D. D. Johnson, Phys. Rev. B **38**, 12807 (1988).
[39] V. Eyert, J. Comput. Phys. **124**, 271 (1996).
[40] A. Baran, A. Bulgac, Michael McNeil Forbes, G. Hagen, W. Nazarewicz, N. Schunck, and M. V. Stoitsov, Phys. Rev. C **78**, 014318 (2008).
[41] L. D. Marks and D. R. Luke, Phys. Rev. B **78**, 075114 (2008).
[42] P. Pulay, Chem. Phys. Lett. **73**, 393 (1980).
[43] G. Kresse and J. Furthmüller, Phys. Rev. B **54**, 11169 (1996).
[44] D. G. Anderson, J. Assoc. Comput. Mach. **12**, 547 (1965).
[45] G. Kresse and J. Furthmüller, Comput. Mater. Sci. **6**, 15 (1996).
[46] P.-M. Anglade and X. Gonze, Phys. Rev. B **78**, 045126 (2008).
[47] D. R. Bowler and M. J. Gillan, Chem. Phys. Lett. **325**, 473 (2000).
[48] P. Bendt and A. Zunger, Phys. Rev. B **26**, 3114 (1982).
[49] P. W. Anderson, Phys. Rev. **124**, 41 (1961).
[50] H. O. Frota and L. N. Oliveira, Phys. Rev. B **33**, 7871 (1986).
[51] V. L. Campo and L. N. Oliveira, Phys. Rev. B **72**, 104432 (2005).
[52] W. C. Oliveira and L. N. Oliveira, Phys. Rev. B **49**, 11986 (1994).
[53] R. Žitko and T. Pruschke, Phys. Rev. B **79**, 085106 (2009).
[54] R. Žitko, Comput. Phys. Commun. **180**, 1271 (2009).
[55] W. Hofstetter, Phys. Rev. Lett. **85**, 1508 (2000).
[56] A. Weichselbaum and J. von Delft, Phys. Rev. Lett. **99**, 076402 (2007).
[57] G. Moeller, Q. Si, G. Kotliar, M. Rozenberg, and D. S. Fisher, Phys. Rev. Lett. **74**, 2082 (1995).
[58] M. Karski, C. Raas, and G. S. Uhrig, Phys. Rev. B **72**, 113110 (2005).
[59] M. Karski, C. Raas, and G. S. Uhrig, Phys. Rev. B **77**, 075116 (2008).
[60] J. Joo and V. Oudovenko, Phys. Rev. B **64**, 193102 (2001).
[61] M. J. Rozenberg, R. Chitra, and G. Kotliar, Phys. Rev. Lett. **83**, 3498 (1999).
[62] L. Laloux, A. Georges, and W. Krauth, Phys. Rev. B **50**, 3092 (1994).
[63] J. Bauer and A. C. Hewson, Phys. Rev. B **76**, 035118 (2007).
[64] D. Vollhardt, Rev. Mod. Phys. **56**, 99 (1984).
[65] J. Spałek and P. Gopalan, Phys. Rev. Lett. **64**, 2823 (1990)
[66] J. Bauer, Eur. Phys. J. B **68**, 201 (2009).
[67] G. Kotliar, Eur. Phys. J. B **11**, 27 (1999).
[68] R. Zitzler, T. Pruschke, and R. Bulla, Eur. Phys. J. B **27**, 473 (2002).
[69] T. Pruschke, Prog. Theor. Phys. **160**, 274 (2005).
[70] R. Peters and T. Pruschke, Phys. Rev. B **76**, 245101 (2007).
[71] M. Potthoff, Eur. Phys. J. B **32**, 429 (2003).